

# Oxide/oxide composites in the system $\text{Cr}_2\text{O}_3\text{-Y}_2\text{O}_3\text{-Al}_2\text{O}_3$

Zhijian Shen, Åsa Ekstrand, Mats Nygren\*

*Department of Inorganic Chemistry, Arrhenius Laboratory Stockholm University, S-106 91 Stockholm, Sweden*

Accepted 18 August 1999

## Abstract

Ceramic compacts in the systems  $\text{Al}_2\text{O}_3\text{-Y}_2\text{O}_3$ ,  $\text{Cr}_2\text{O}_3\text{-Y}_2\text{O}_3$  and  $\text{Y}_3(\text{Cr}_y\text{Al}_{1-y})_5\text{O}_{12}$  (Cr-doped YAG) were prepared by solid state reaction in calcined co-precipitated powder mixtures of appropriate compositions. Various solid-solution phases were formed, e.g.  $\text{Y}_3(\text{Al}_{1-x}\text{Cr}_x)_5\text{O}_{12}$ ,  $\text{YAl}_y\text{Cr}_{1-y}\text{O}_3$  and  $\text{Al}_{2-x}\text{Cr}_x\text{O}_3$ . Composite materials in the pseudo-binary or ternary systems  $\text{Al}_2\text{O}_3\text{-Y}_3\text{Al}_5\text{O}_{12}$ ,  $\text{Cr}_2\text{O}_3\text{-Y}_2\text{O}_3$  and  $\text{Y}_3(\text{Al}_{1-x}\text{Cr}_x)_5\text{O}_{12}\text{-YAl}_y\text{Cr}_{1-y}\text{O}_3\text{-(Al}_2\text{Cr}_{1-z})_2\text{O}_3$  were obtained by hot-pressing appropriate powder precursors at 1600–1650°C for 1 h. The microstructure of the prepared materials was studied in a scanning electron microscope with element analysis facilities. X-ray diffraction was used to reveal the phases present and their lattice parameters. The chemical compatibility of these phases was investigated. The results are discussed with a special emphasis on the solubility of Cr in the YAG structure, and on the compatibility relationship between Cr-doped YAG and its neighbouring phases. A gel-coating process for preparing  $\text{Al}_2\text{O}_3\text{-YAG}$  composites with tailored microstructures is also described. © 2000 Elsevier Science Ltd. All rights reserved.

*Keywords:*  $\text{Al}_2\text{O}_3\text{-Y}_2\text{O}_3$ ; Composites;  $\text{Cr}_2\text{O}_3\text{-Y}_2\text{O}_3$ ; Hot pressing; Microstructure-final; YAG

## 1. Introduction

It is by now well recognised that oxide-based materials are the only ones which can survive in oxidising environments for any length of time at temperatures approaching or exceeding of 1400°C. However, most monophasic polycrystalline oxide ceramic compacts can not be used at elevated temperatures ( $T > 1000^\circ\text{C}$ ) due to: (i) their inherent brittleness; (ii) loss of strength due to grain growth; (iii) grain boundary dominated creep. Accordingly, the idea of developing duplex or multiphase oxide/oxide-based composites exhibiting enhanced oxidation- and creep-resistant properties have become attractive.

The oxide components chosen must, of course, also be chemically compatible and have adequate thermal stability to prevent mechanical degradation. Previous studies have identified the  $\text{Y}_3\text{Al}_5\text{O}_{12}$  (YAG)– $\text{Al}_2\text{O}_3$  system to be of interest.<sup>1–3</sup> YAG is compatible with  $\alpha\text{-Al}_2\text{O}_3$  because these two phases have similar thermal expansion coefficients and both have high melting temperatures, namely 1940 and 2045°C for YAG and  $\text{Al}_2\text{O}_3$ , respectively.<sup>4</sup> Furthermore, YAG retains its bend strength up to 1400°C, and exhibits high creep resistance at elevated temperatures.<sup>5,6</sup>

It has been noticed that the creep behaviour of polycrystalline oxide compacts is most often dominated by grain-boundary diffusion. The creep strength of monolithic oxide compacts might thus be improved by a moderate addition of a secondary oxide phase, yielding a biphasic oxide composite with duplex morphology. Further improvement of the creep strength might also be achieved by the formation of solid solutions such as  $\text{Y}_3(\text{Al}_{1-x}\text{Cr}_x)_5\text{O}_{12}$  in combination with the incorporation of second-phase oxide particles in the grain boundaries of the parent garnet oxide phase.

In order to identify factors which might influence the high-temperature creep behaviour, e.g. grain size and morphology, formation of solid solutions, particle inclusions at the grain boundaries, etc., composite materials in the system  $\text{Cr}_2\text{O}_3\text{-Y}_2\text{O}_3\text{-Al}_2\text{O}_3$  have been studied in some detail. In this presentation, we will focus on the solubility of Cr in the YAG structure, and on the compatibility relationship of Cr-doped YAG with its neighbouring phases. We will also emphasise processes designed to approach designed structures such as duplex microstructures of micron-sized uniformly mixed particles of  $\text{Al}_2\text{O}_3$  and YAG covering a wide range of volume fractions of each component. The creep behaviour of the prepared composite materials will be discussed in a forthcoming article.

\* Corresponding author. Tel.: +46-8-162366.

## 2. Experimental

Two series of samples were prepared, the first one with overall compositions  $Y_3(Al_{1-x}Cr_x)_5O_{12}$  ( $0 \leq x \leq 1$ ), located on the line joining the two nominal compositions  $3Y_2O_3 \cdot 5Al_2O_3$  and  $3Y_2O_3 \cdot 5Cr_2O_3$ . The second series covered the pseudo-binary system  $Y_3Al_5O_{12}-Al_2O_3$ , yielding compacts with a variety of phase fractions of  $Y_3Al_5O_{12}$  and  $Al_2O_3$  and microstructural morphologies. In the former series, the powder mixtures were prepared from aqueous solution by a co-precipitation route, i.e. by addition of  $NH_3(aq)$  to an aqueous solution containing appropriate amounts of  $Al(NO_3)_3$ ,  $YCl_3$  and  $Cr(NO_3)_3$ , as outlined in Fig. 1(a). In the latter series, the powder mixtures were prepared by a gel-coating process, using aluminium acetate [ $Al(OAc)_3$  abbreviated AAT below] dissolved in an acetic acid: methanol solution (1:1 by volume) as precursor for  $Al_2O_3$ . An appropriate commercially available sub-microsized YAG-powder was added to this solution. In

order to prevent  $Al(OAc)_3 \cdot 0.5H_2O$  from precipitating when the AAT solution containing the YAG particles was evaporated, we added 1 mol of triethyl-amine (TEA) per mol of  $Al^{3+}$ . The TEA molecule partly replaces some OAc-groups in  $Al(OAc)_3$  thereby forestalling the crystallisation of  $Al(OAc)_3 \cdot 0.5H_2O$ . The process is outlined in Fig. 1(b). In addition, an yttrium-aluminium-acetate solution of the YAG composition was used for preparation of precursor mixtures having  $Al_2O_3$  as matrix material, with minor additions of YAG intended to act as  $Al_2O_3$  grain growth inhibitor.

The burning-off of the gels was monitored by thermogravimetric analysis, and the produced crystalline powder precursors were investigated, with respect to phase formation and composition, by X-ray powder diffraction (XRD) and scanning electron microscopy (SEM; Jeol JSM 880, equipped with energy-dispersive spectrometer, EDS; Link AN 10 000). The obtained powder mixtures in the systems of  $Y_3(Al_{1-x}Cr_x)_5O_{12}$  and  $Y_3Al_5O_{12}-Al_2O_3$  were densified by hot-pressing for 1 h in Ar at 1600 and 1650°C, respectively. Polished and thermally etched (1500°C/30min in air) samples were examined by SEM/EDS to reveal their microstructures. Density measurement together with microstructure investigation revealed that the obtained samples were all fully densified. The overall compositions and phase contents of samples prepared in system  $Y_3(Al_{1-x}Cr_x)_5O_{12}$  are listed in Table 1, where the composition of various phases were determined by EDS analyses and the phase contents were obtained by combining quantitative XRD analyses and weight-balance calculations.

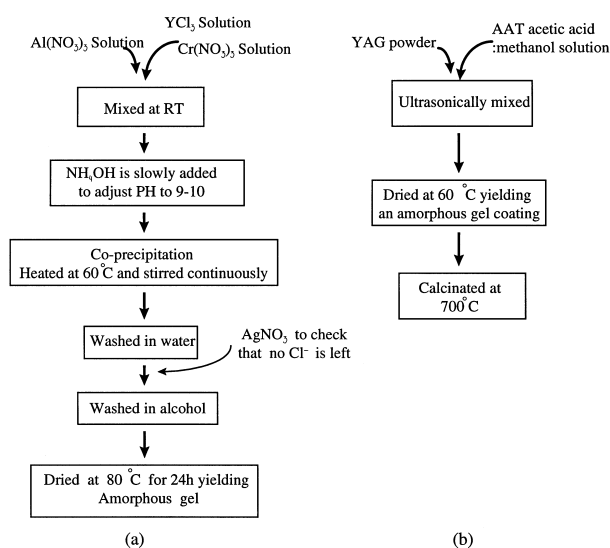


Fig. 1. Schematic presentation of (a) the co-precipitation route and (b) the gel-coating process, for preparing precursor mixtures to  $Y_3(Al_{1-x}Cr_x)_5O_{12}$  with  $0 \leq x \leq 1$  and to samples in the  $Y_3Al_5O_{12}-Al_2O_3$  system, respectively.

## 3. Results and Discussion

### 3.1. The solid solubility limit of Cr in the YAG structure

Fig. 2. shows the XRD patterns of samples prepared in the  $Y_3(Al_{1-x}Cr_x)_5O_{12}$  system. From this figure and Table 1 it is obvious that the obtained phase assemblages in this series vary with the nominal sample composition. Three phases form in this system, namely a Cr-doped garnet solid solution,  $Y_3(Al_{1-x}Cr_x)_5O_{12}$ , an

Table 1  
Phase content of  $Y_3(Al_{1-x}Cr_x)_5O_{12}$  samples densified at 1600°C for 1 h

Sample label	Overall composition	Amount of (wt%)		
		$Y_3(Cr_xAl_{1-x})_5O_{12}$	$YAl_yCr_{1-y}O_3$	$Al_{2-x}Cr_xO_3$
YAG	$3Y_2O_3 \cdot 5Al_2O_3$	$x = 0$ , 100%	–	–
CYG02	$Y_3(Cr_{0.2}Al_{0.8})_5O_{12}$	$x = 0.2$ , 100%	–	–
CYG04	$Y_3(Cr_{0.4}Al_{0.6})_5O_{12}$	$x = 0.25$ , 66.0%	$y = 0.25$ , 27.3%	$x = 1.35$ , 6.7%
CYG06	$Y_3(Cr_{0.6}Al_{0.4})_5O_{12}$	$x = 0.27$ , 21.6%	$y = 0.23$ , 63.3%	$x = 1.2$ , 15.1%
CYG08	$Y_3(Cr_{0.8}Al_{0.2})_5O_{12}$	–	$y = 0.20$ , 79.5%	$x = 1.6$ , 20.5%
CYG10	$3Y_2O_3 \cdot 5Cr_2O_3$	–	$y = 0$ , 78.9%	$x = 2$ , 21.1%

Al-doped chromium–yttrium oxide,  $YAl_yCr_{1-y}O_3$ , and an Al-doped chromium oxide,  $Al_{2-x}Cr_xO_3$ . To give an even better overview, the back-scattering SEM micrographs, obtained in BSE mode, of a series of samples

are given in Fig. 3. The grey, white and black grains represent the  $Y_3(Al_{1-x}Cr_x)_5O_{12}$ ,  $YAl_yCr_{1-y}O_3$  and  $Al_{2-x}Cr_xO_3$  phases, respectively. The monophasic samples YAG and CYG02 have been thermally etched in order to reveal the grain boundaries.

The solubility limit of Cr in  $Y_3(Al_{1-x}Cr_x)_5O_{12}$  was determined by XRD and EDS analysis of individual grains. The lattice parameters of the YAG unit cell are plotted in Fig. 4. versus the  $x$ -value deduced from the EDS analysis. From this figure it can be concluded that the solubility limit of Cr in  $Y_3(Al_{1-x}Cr_x)_5O_{12}$  is around  $x = 0.25$ .

### 3.2. The compatibility relationship of Cr-doped YAG with its neighbouring phases

Three compounds have been reported in the system  $Y_2O_3-Al_2O_3$ :  $Y_3Al_5O_{12}$  with the garnet structure (YAG),  $Y_4Al_2O_9$  with a monoclinic structure (YAM), and  $YAlO_3$  with the perovskite structure (YAP). The first two are stable, whereas the third one is reported to be metastable.<sup>4,7,8</sup>  $YCrO_3$  with the perovskite structure is the only compound found in the system  $Y_2O_3-Cr_2O_3$ .<sup>9</sup>

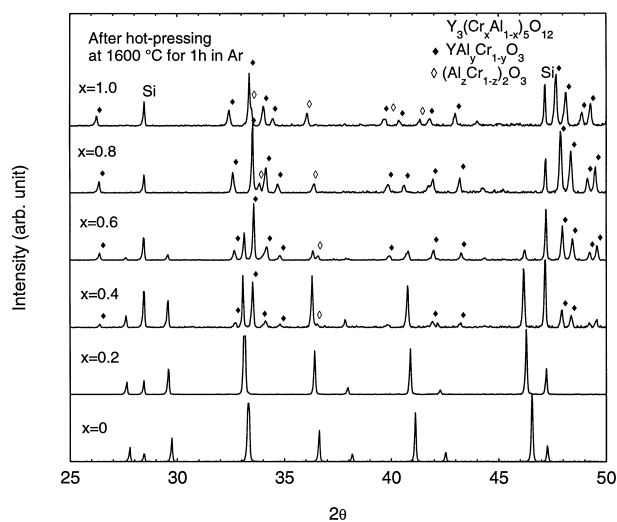


Fig. 2. XRD patterns of the  $Y_3(Al_{1-x}Cr_x)_5O_{12}$  samples.

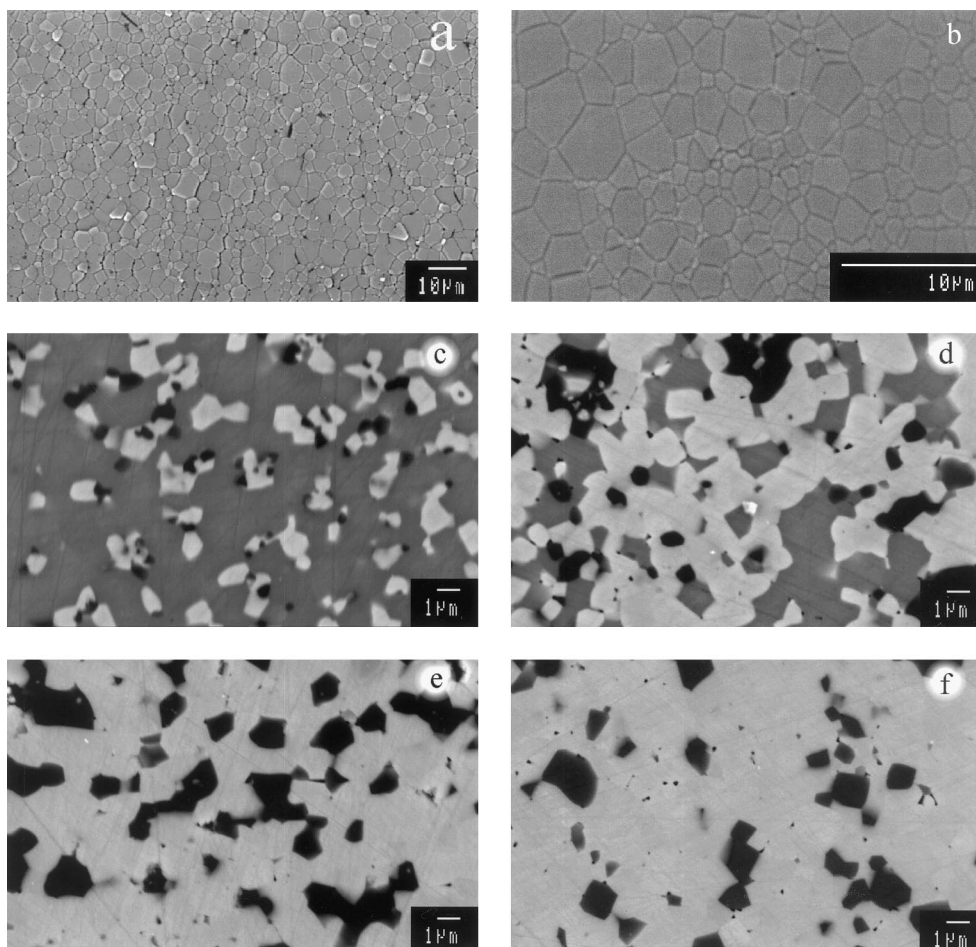
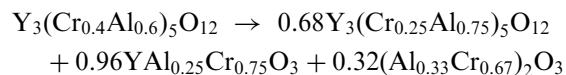


Fig. 3. Microstructures of the  $Y_3(Al_{1-x}Cr_x)_5O_{12}$  samples: (a) YAG; (b) CYG02; (c) CYG04; (d) CYG06; (e) CYG08; (f) CYG10.

In the system  $\text{Al}_2\text{O}_3\text{--Cr}_2\text{O}_3$ , a continuous solid solution  $\text{Al}_{2-x}\text{Cr}_x\text{O}_3$  with  $0 \leq x \leq 2$  has been reported.<sup>10</sup>

Compacts of the nominal composition  $\text{Y}_3(\text{Al}_{1-x}\text{Cr}_x)_5\text{O}_{12}$  with  $0 \leq x \leq 1$  were monophasic for  $x \leq 0.25$  (see Table 1 and Fig. 4), while for  $x = 0.4$  and  $0.6$  the phases  $\text{YAl}_y\text{Cr}_{1-y}\text{O}_3$  with  $y = 0.23\text{--}0.25$  and  $\text{Al}_{2-x}\text{Cr}_x\text{O}_3$  with  $x = 1.2\text{--}1.3$  were formed together with the garnet phase of the composition  $\text{Y}_3(\text{Al}_{1-x}\text{Cr}_x)_5\text{O}_{12}$  with  $x = 0.25$  (see also Fig. 5). No garnet phase was formed in samples with  $x \geq 0.8$ , but a mixture of the phases  $\text{YAl}_y\text{Cr}_{1-y}\text{O}_3$  and  $\text{Al}_{2-x}\text{Cr}_x\text{O}_3$  was found.

The reactions in samples of the nominal composition  $\text{Y}_3(\text{Al}_{1-x}\text{Cr}_x)_5\text{O}_{12}$  with  $x \geq 0.4$  can thus be delineated as: For  $x = 0.4$ :



For  $x = 0.6$ :

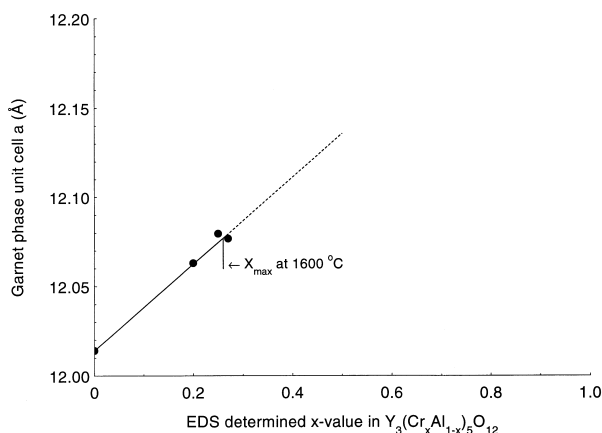
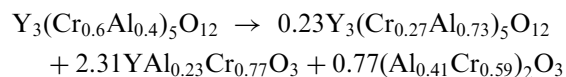


Fig. 4. The lattice parameter of the garnet phase plotted versus the EDS-determined  $x$ -value in the formula  $\text{Y}_3(\text{Al}_{1-x}\text{Cr}_x)_5\text{O}_{12}$ .

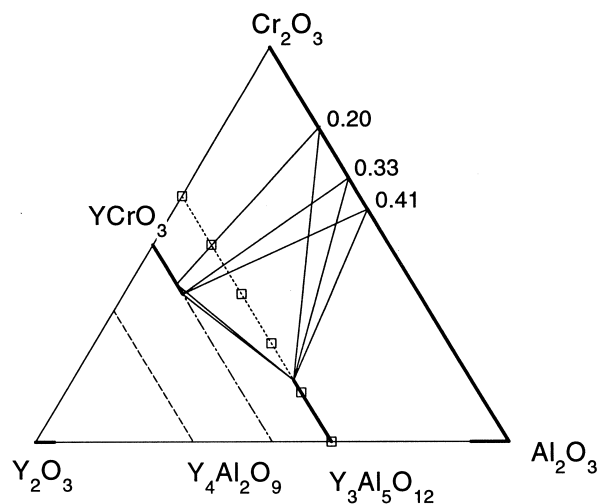
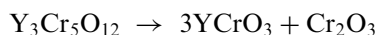


Fig. 5. A schematic phase diagram of the system  $\text{Y}_3(\text{Al}_{1-x}\text{Cr}_x)_5\text{O}_{12}$  with  $0 \leq x \leq 1$  at  $1600^\circ\text{C}$ .

For  $x = 0.8$ :



For  $x = 1.0$



The Cr-doped YAG is chemically incompatible with  $\text{Al}_2\text{O}_3$ , as the following experiment shows: The monophasic Cr-doped YAG compact (CYG02) was crushed and this powder mixed with  $\text{Al}_2\text{O}_3$  powder. A new compact containing 10 vol% of the garnet phase was prepared by hot-pressing at  $1600^\circ\text{C}$  for 1 h in argon. Fig. 6 shows the XRD pattern of this compact. It is evident that the strongest garnet (420) diffraction reflection, at a  $2\theta$  value of  $33.2\text{--}33.3$ , degrees is split into a double peak, indicating that part of the Cr-doped YAG phase has shifted its composition. The SEM micrograph of the compact, recorded in BSE mode, is given in Fig. 7, where the white and black phases are garnet and  $\text{Al}_2\text{O}_3$ , respectively. EDS analysis of individual grains of the Cr-doped YAG phase confirmed that the garnet phase has lost part of its Cr content, which in turn had entered into the  $\text{Al}_2\text{O}_3$  grains located around the garnet grains. The following reaction was thus concluded

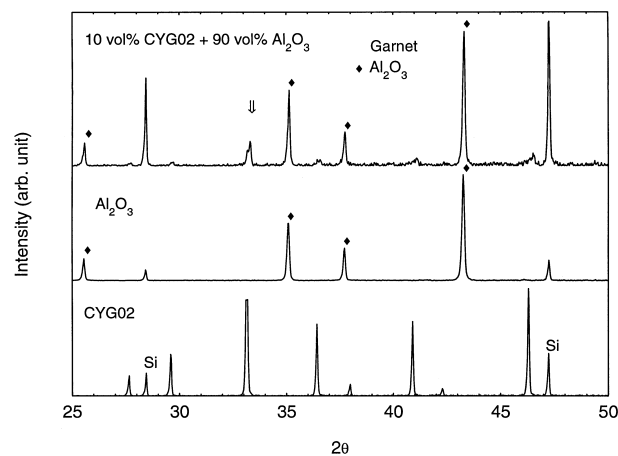


Fig. 6. The XRD pattern of the prepared composite CYG02/ $\text{Al}_2\text{O}_3$ .

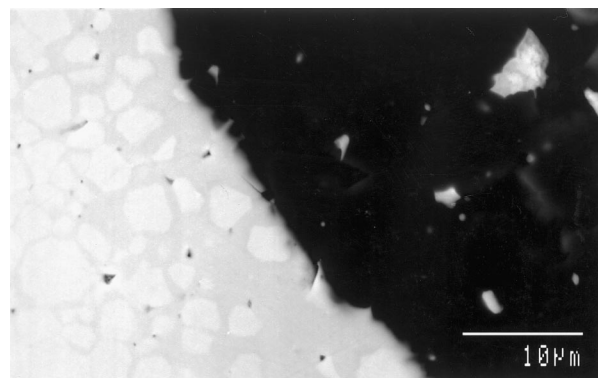


Fig. 7. SEM micrographs recorded in BSE mode of the composite CYG02/ $\text{Al}_2\text{O}_3$ .

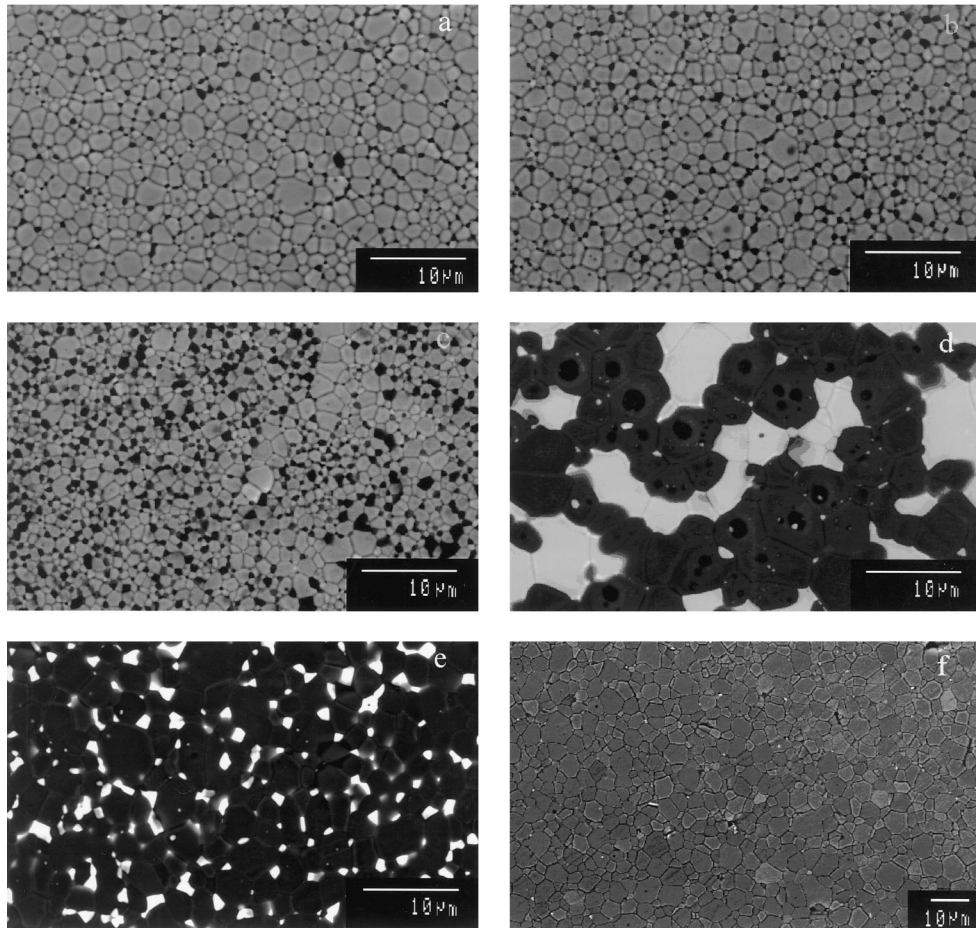
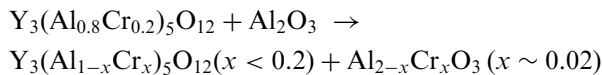


Fig. 8. SEM micrographs of a series of  $\text{Al}_2\text{O}_3/\text{YAG}$  composites prepared from precursor powder mixtures, obtained by the gel-coating process shown in Fig. 1(b), by hot-pressing at  $1650^\circ\text{C}$  for 1 h: (a) 97.5 vol% YAG, (b) 95 vol% YAG, (c) 85 vol% YAG, (d) 54.7 vol% YAG, (e) 12 vol% YAG, (f)  $\text{Al}_2\text{O}_3$ . Refer to Fig. 3(a) for micrograph of pure YAG.

to take place between Cr-doped YAG and  $\text{Al}_2\text{O}_3$  during the sintering process:



### 3.3. Tailoring the microstructure of the composites in the pseudo-binary $\text{Al}_2\text{O}_3\text{--Y}_3\text{Al}_5\text{O}_{12}$ system

In the pseudo-binary  $\text{Al}_2\text{O}_3\text{--YAG}$  system, composites can for example be prepared either by directional solidification of melts or by sintering of  $\text{Al}_2\text{O}_3$  and YAG powder mixtures. Using the gel-coating process illustrated in Fig. 1(b), a series of  $\text{Al}_2\text{O}_3/\text{YAG}$  composites were prepared, with overall compositions close to the YAG and  $\text{Al}_2\text{O}_3$ -rich ends. After hot-pressing at  $1650^\circ\text{C}$  for 1 h, the microstructures of the fully dense compacts consisted of uniformly dispersed micron-sized and equiaxed  $\text{Al}_2\text{O}_3$  grains in a matrix of equiaxed YAG-grains, and vice versa, as seen Fig. 8 (the phases with white and black contrast are YAG and  $\text{Al}_2\text{O}_3$ , respectively). It is

obvious that the addition of even a very small amount of  $\text{Al}_2\text{O}_3$  to the YAG matrix, and vice versa, prevents the growth of the matrix grains. Using this procedure, composite materials containing less than 25 vol% of  $\text{Al}_2\text{O}_3$  and YAG, respectively, yielded homogeneous microstructures, i.e. uniformly dispersed micron-sized and equiaxed alumina grains in a matrix consisting of equiaxed YAG-grains, and vice versa. It should be pointed out that a drawback of the gel-coating process described in Fig. 1(b) is that it is impossible to avoid formation of agglomerates of both  $\text{Al}_2\text{O}_3$  and YAG grains in composites containing 25–75 vol% of the matrix phase.

## 4. Conclusions

The following conclusions can be drawn:

1. The substitution limit of Cr for Al in the Y–Al garnet phase (YAG) is  $\approx 25$  mol% at  $1600^\circ\text{C}$ , i.e.  $x \approx 0.25$  in  $\text{Y}_3(\text{Al}_{1-x}\text{Cr}_x)_5\text{O}_{12}$ .

- Cr-doped YAG,  $Y_3(Al_{1-x}Cr_x)_5O_{12}$ , reacts with  $Al_2O_3$  to form  $YAl_yCr_{1-y}O_3$  and  $Al_{2-x}Cr_xO_3$ , i.e.  $Y_3(Al_{1-x}Cr_x)_5O_{12}$  is incompatible with  $Al_2O_3$ .
- The microstructures of  $Al_2O_3$ /YAG composites with overall compositions close to the YAG and  $Al_2O_3$ -rich ends, respectively, consist of uniformly dispersed micron-sized and equi-axed  $Al_2O_3$  grains in a matrix of equi-axed YAG-grains, and vice versa.

### Acknowledgements

We thank Andreas Flemström for his assistance with the preparation of the  $Al_2O_3$ /YAG composites. This work has been financially supported by the EC BRITE-EURAM contract BRPR-CT95-0110.

### References

- Mah, T., Parthasarathy, T. A. and Matson, L. E., Processing and mechanical properties of  $Al_2O_3/Y_3Al_5O_{12}$  (YAG) eutectic composite. *Ceram. Eng. Sci. Proc.*, 1990, **11**, 1617–1627.
- Parthasarathy, T. A., Mah, T. and Matson, L. E., Creep behavior of an  $Al_2O_3-Y_3Al_5O_{12}$  eutectic composite. *Ceram. Eng. Sci. Proc.*, 1990, **11**, 1628–1638.
- Matson, L. E., Hay, R. S. and Mah, T., Characterization of alumina/ytterium–aluminum garnet and alumina/ytterium–aluminum perovskite eutectics. *Ceram. Eng. Sci. Proc.*, 1990, **11**, 995–1003.
- Mah, T. and Petry, M. D., Eutectic composition in the pseudobinary of  $Y_4Al_2O_9$  and  $Y_2O_3$ . *J. Am. Ceram. Soc.*, 1992, **75**, 2006–2009.
- Corman, G. S., Creep of ytterium aluminium garnet single crystals. *J. Mater. Sci. Letters*, 1993, **12**, 379–382.
- Parthasarathy, T. A., Mah, T. and Keller, K., Creep mechanism of polycrystalline ytterium aluminum garnet. *J. Am Ceram. Soc.*, 1992, **75**, 1756–1759.
- Cockayne, B., The use and enigma of the  $Al_2O_3-Y_2O_3$  phase system. *J. Less-Common Met.*, 1985, **114**, 199–206.
- Caslavsk, J. L. and Viechnicki, D. J., Melting behavior and metastability of ytterium aluminum garnet (YAG) and  $YAlO_3$  determined by optical differential thermal analysis. *J. Mater. Sci.*, 1980, **15**, 1709–1718.
- Pavlikov, V.N., Shevchenko, A.V., Lopato, L.M. and Tresvyatskii S.G., In *Chemistry of High Temperature Materials*, ed. N. A. Toropov (transl. by C.B. Finch). Consultants Bureau, New York, 1969.
- Watanabe, M., Hirayama, T., Yoshinaka, M., Hirata, K. and Yamaguchi, O., Formation of continuous series of solid solutions from powders prepared by hydrazine method: the system  $Cr_2O_3-Al_2O_3$ . *Mater. Res. Bull.*, 1996, **31**, 861–868.